Available online at www.sciencedirect.com
ScienceDirect
Trans. Nonferrous Met. Soc. China 21(2011) 467−476
Transactions of Nonferrous Metals Society of China
www.tnmsc.cn

Optimization of pulsed current gas tungsten arc welding process parameters to attain maximum tensile strength in AZ31B magnesium alloy

G. PADMANABAN, V. BALASUBRAMANIAN

Center for Materials Joining and Research (CEMAJOR), Department of Manufacturing Engineering, Annamalai University, Annamalainagar−608 002, Tamil Nadu, India

Received 7 May 2010; accepted 22 July 2011

Abstract: An empirical relationship to predict tensile strength of pulsed current gas tungsten arc welded AZ31B magnesium alloy was developed. Incorporating process parameters such as peak current, base current, pulse frequency and pulse on time were studied. The experiments were conducted based on a four-factor, five-level, central composite design matrix. The developed empirical relationship can be effectively used to predict the tensile strength of pulsed current gas tungsten arc welded AZ31B magnesium alloy joints at 95% confidence level. The results indicate that pulse frequency has the greatest influence on tensile strength, followed by peak current, pulse on time and base current.

Key words: AZ31B magnesium alloy; pulsed current gas tungsten arc welding; response surface methodology; optimization; tensile strength

1 Introduction

In recent years, magnesium and its alloys have attracted great attention in academic research and industry applications, due to their low density and recyclability. Especially in automotive industry, mass reduction through replacing steel and aluminum parts is an important factor in reducing fuel consumption. Therefore, magnesium and its alloys are considered one of the most promising basic materials in the 21st century. However, the development of new manufacturing techniques plays an important role in exploiting new magnesium alloys in new fields of applications. Recently, the interest on welding of magnesium alloys has been increasing rapidly, mainly focusing on gas tungsten arc welding (GTAW), laser-beam welding, electron beam welding and friction-stir welding[1−3].

GTAW is a widely used material joining process, especially for nonferrous lightweight metals such as magnesium, aluminum and titanium. The quality of GTA welds ranks higher than that of other arc-welding processes, due to the reliability, clearance and strength of the weld. For magnesium alloy, alternating current (AC) offers a major advantage of cathodic cleaning of the magnesia covering the surfaces over direct current (DC) to initiate a weld pool. However, compared to DC where the electrode is anode and workpiece is cathode, AC lowers the heat input to the base metal and produces shallower welds, especially when argon is selected over helium. Plasma arc welding process can be used as an alternative of the GTAW process, allowing a high welding penetration. However, plasma arc welding is much more complex and presents greater initial and operational costs than the GTAW process. For the advantages of utility and economy, GTAW has been used extensively. Pulsed current gas tungsten arc welding (PCGTAW) is a variation of GTA welding which involves cycling of the welding current from a high level to a low level at a selected regular frequency[4−5].

In welding processes, the input parameters have greater influence on the mechanical properties of the welded joints. By varying the input process parameters, the output could be changed with significant variation in their mechanical properties. Accordingly, welding is usually selected to get a welded joint with excellent mechanical properties. To determine these welding combinations that would lead to excellent mechanical properties, different methods and approaches have been

Corresponding author: G. PADMANABAN; Tel: +91-4144-239743; Fax: +91-4144-2308080; E-mail: gknaban@rediffmail.com
DOI: 10.1016/S1003-6326(11)60738-3

used. Various optimization methods can be applied to define the desired output variables through developing mathematical models to specify the relationship between the input parameters and output variables. One of the most widely used methods to solve this problem is response surface methodology (RSM), in which the unknown mechanism with an appropriate empirical model is approximated, being the function of representing a response surface model[6].

Several studies reported[7−10] the effect of pulsed current gas tungsten arc welding process parameters on mechanical and metallurgical properties of AZ31B magnesium alloy. However, there is no information on the prediction of optimum pulsed current GTAW process parameters to attain maximum tensile strength in AZ31B magnesium alloy joints. In this investigation, an attempt was made to develop an empirical relationship to predict the tensile strength of pulsed current gas tungsten arc welded AZ31B magnesium alloy joints using statistical tools such as design of experiments, analysis of variance and regression analysis. Attempt was also extended to optimize the PCGTAW process parameters to attain maximum tensile strength of AZ31B magnesium alloy.

2 Development of empirical relationship

2.1 Important parameters

From Refs.[8, 11] and preliminary work done in our laboratory, the predominant factors of peak current, base current, pulse frequency and pulse on time which have great influence on the tensile strength of pulsed current GTA welded joints were identified.

2.2 Working limits of parameters

The composition and mechanical properties of the base metal are listed in Tables 1 and 2, respectively. A large number of trial runs were carried out using 6 mm thick rolled plates of AZ31B magnesium alloy to find out feasible working limits of pulsed current GTAW parameters. Different combinations of pulsed current parameters were used to carry out the trial runs. The bead contour, bead appearance and weld quality were inspected to identify the working limits of the welding parameters, leading to the following observations. 1) If the peak current was less than 190 A, there were incomplete penetration and lack of fusion. For peak current greater than 230 A, undercut and spatter were observed on the weld bead surface. 2) If the base current was lower than 60 A, the arc length was found to be short. For base current greater than 100 A, the arc becomes unstable and the arc wandering was observed due to increased arc length. 3) If the pulse frequency was lower than 2 Hz, the bead appearance and contours were comparable to those of constant current weld beads. When the frequency was greater than 10 Hz, more arc glare and arc spatter were observed. 4) If pulse on-time was lower than 40%, the weld bead formation was not smooth. When it was greater than 60%, overheating of tungsten electrode was noticed.

Table 1 Chemical composition of base metal AZ31B magnesium alloy (mass fraction, %)

Al	Mn	Zn	Mg
3.0	0.20	1.0	Bal.

Table 2 Mechanical properties of base metal AZ31B magnesium alloy

Yield strength/MPa	Ultimate tensile strength/MPa	Elongation/%	Reduction/%	Hardness (Hv)
171	215	14.7	14.3	69.3

2.3 Development of design matrix

By considering all the conditions above, feasible limits of the parameters were chosen in a way that the AZ31B magnesium alloy should be welded without any weld defects. Among a wide range of factors, four factors and five levels central composite design matrix were selected to optimize the experimental conditions. Table 3 presents the range of factors considered and Table 4 shows 31 sets of coded conditions used to form the design matrix. The method of designing such matrix is introduced elsewhere[12]. For the convenience of recording and processing experimental data, upper and lower levels of the factors were coded as +2 and −2, respectively.

Table 3 Important PCGTAW parameters and their working range

Parameter	Notation	Level				
		−2	−1	0	+1	+2
Peak current/A	P	190	200	210	220	230
Base current/A	B	60	70	80	90	100
Pulse frequency/Hz	F	2	4	6	8	10
Pulse on time/%	T	40	45	50	55	60

2.4 Experiments

Rolled plates of AZ31B magnesium alloy of 6 mm thickness of were cut into required size of 300 mm×150 mm×6 mm by machining, as shown in Fig.1. Square butt joint configuration was prepared to fabricate PCGTAW joints. The initial joint configuration was obtained by securing the plates in position using mechanical clamps. The direction of welding was normal to the rolling direction. Single pass welding procedure was used to fabricate the joints. Argon (purity 99.99%) was used as shielding gas. A constant welding speed of 2.5 mm/s was used in this investigation.

The fabricated joints were sliced and then machined to a required size, as shown in Fig.2, according to ASTM E8M-04 standard for sheet type material. The smooth (unnotched) tensile specimens were prepared to evaluate the tensile strength. Photos of fabricated joints and samples are shown in Fig.3. Tensile test was carried out in an electro-mechanical controlled universal testing machine (FIE-Bluestar, UNITEK−94100) and the average values of three results are presented in Table 4.

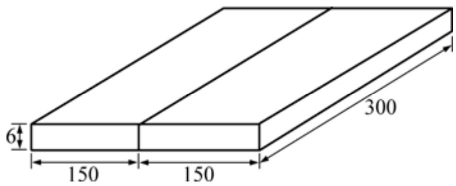

Fig.1 Dimensions of joint configuration (Unit: mm)

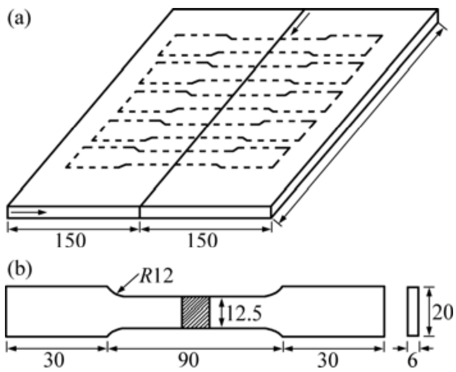

Fig.2 Dimensions of tensile specimen: (a) Schematic diagram of welding with respect to rolling direction and extraction of tensile specimens; (b) Dimensions of flat smooth tensile specimen

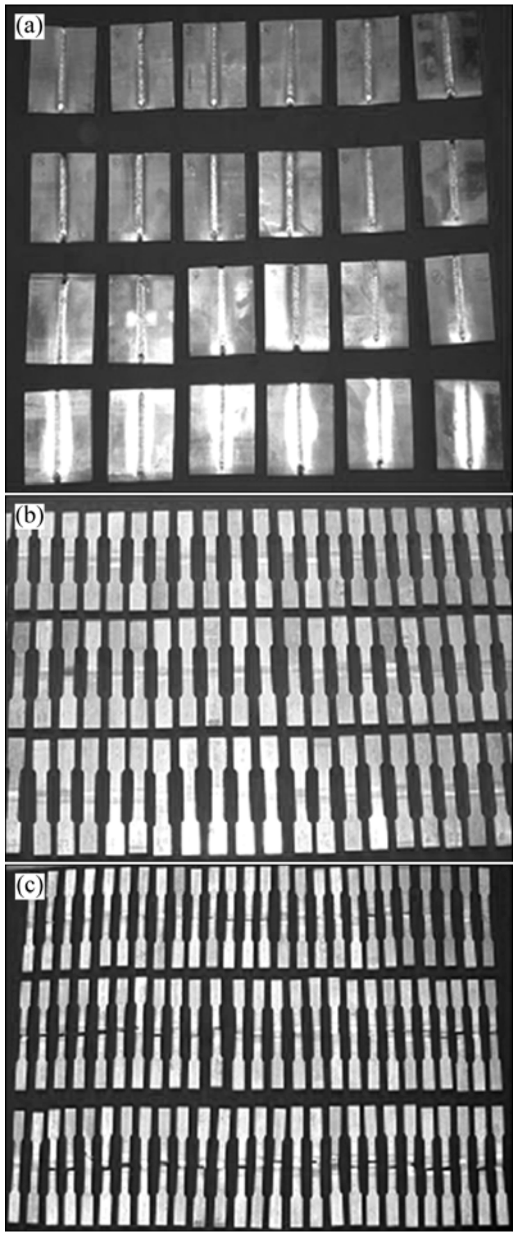

Fig.3 Photographs of fabricated joints and tensile specimens: (a) Fabricated joints; (b) Tensile specimens (before tensile test); (c) Tensile specimens (after tensile test)

2.5 Development of empirical relationship

Response surface methodology (RSM) is a collection of mathematical and statistical techniques that is useful for modeling and analyzing problems, in which a response of interest is influenced by several variables and the objective is to optimize this response. The response function of the joint, tensile strength (σ), is a function of peak current (P), base current (B), pulse frequency (F) and pulse on time (T), and it can be expressed as:

$$\sigma=f(P,\ B,\ F,\ T) \tag{1}$$

The second order polynomial (regression) equation used to represent the response surface 'Y' is given as:

$$Y=b_0+\sum b_i x_i+\sum b_{ii} x_i^2+\sum b_{ij} x_i x_j+e_r \tag{2}$$

and for four factors, the selected polynomial could be expressed as:

$$\begin{aligned}\sigma=&b_0+b_1(P)+b_2(B)+b_3(F)+b_4(T)+b_{11}(P^2)+b_{22}(B^2)+\\&b_{33}(F^2)+b_{44}(T^2)+b_{12}(PB)+b_{13}(PF)+b_{14}(PT)+\\&b_{23}(BF)+b_{24}(BT)+b_{34}(FT)\end{aligned} \tag{3}$$

where b_0 is the average of responses; b_i and b_{ij} are the coefficients that depend on the respective main and interaction effects of the parameters.

In order to estimate the regression coefficients, a number of experimental design techniques are available. In this work, central composite design which accurately fits the second order response surface was used. All the coefficients were obtained by applying central composite design using the Design Expert statistical software package. After determining significant coefficients, the final relationship was developed using only these coefficients. The empirical relationship to predict tensile strength of pulsed current gas tungsten arc welded AZ31B magnesium alloy is given as:

Table 4 Design matrix and experimental results

Exp. No	Coded value P	B	F	T	Actual value P/A	B/A	F/Hz	T/%	Tensile strength/ MPa
1	−1	−1	−1	−1	200	70	4	45	172
2	+1	−1	−1	−1	220	70	4	45	168
3	−1	+1	−1	−1	200	90	4	45	178
4	+1	+1	−1	−1	220	90	4	45	172
5	−1	−1	+1	−1	200	70	8	45	182
6	+1	−1	+1	−1	220	70	8	45	170
7	−1	+1	+1	−1	200	90	8	45	183
8	+1	+1	+1	−1	220	90	8	45	169
9	−1	−1	−1	+1	200	70	4	55	157
10	+1	−1	−1	+1	220	70	4	55	160
11	−1	+1	−1	+1	200	90	4	55	166
12	+1	+1	−1	+1	220	90	4	55	167
13	−1	−1	+1	+1	200	70	8	55	176
14	+1	−1	+1	+1	220	70	8	55	169
15	−1	+1	+1	+1	200	90	8	55	179
16	+1	+1	+1	+1	220	90	8	55	169
17	−2	0	0	0	190	80	6	50	178
18	+2	0	0	0	230	80	6	50	163
19	0	−2	0	0	210	60	6	50	162
20	0	+2	0	0	210	100	6	50	170
21	0	0	−2	0	210	80	2	50	167
22	0	0	+2	0	210	80	10	50	182
23	0	0	0	−2	210	80	6	40	177
24	0	0	0	+2	210	80	6	60	168
25	0	0	0	0	210	80	6	50	186
26	0	0	0	0	210	80	6	50	186
27	0	0	0	0	210	80	6	50	188
28	0	0	0	0	210	80	6	50	188
29	0	0	0	0	210	80	6	50	187
30	0	0	0	0	210	80	6	50	188
31	0	0	0	0	210	80	6	50	188

$$\sigma=187.17-3.29(P)+1.87(B)+3.62(F)-2.88(T)-0.56(PB)-2.31(PF)+1.44(PT)-1.44(BF)+0.56(BT)+1.81(FT)-4.14(P^2)-5.26(B^2)-3.14(F^2)-3.64(T^2) \quad (4)$$

2.6 Checking adequacy of developed relationship

The adequacy of the developed relationship was tested using the analysis of variance technique (ANOVA). In this technique, if the calculated F_{ratio} value of the developed model is less than the standard F_{ratio} (from F-table) value at a desired level of confidence (95%), the model is adequate within the confidence limit. The ANOVA test results are presented in Table 5. It is understood that the developed relationship is adequate at 95% confidence level.

Table 5 ANOVA test results

Source	Sum of squares	df	Mean square	F value	P-value Prob >F
Model	2406.45	14	171.89	172.85	<0.0001
P-P	260.04	1	260.04	261.49	<0.0001
B-B	84.38	1	84.38	84.85	<0.0001
F-F	315.38	1	315.38	317.14	<0.0001
T-T	198.38	1	198.38	199.48	<0.0001
PB	5.06	1	5.06	5.09	0.0394
PF	85.56	1	85.56	86.04	<0.0001
PT	33.06	1	33.06	33.24	<0.0001
BF	33.06	1	33.06	33.24	<0.0001
BT	5.06	1	5.06	5.09	0.0394
FT	52.56	1	52.56	52.86	<0.0001
P^2	469.07	1	469.07	471.69	<0.0001
B^2	759.01	1	759.01	763.24	<0.0001
F^2	269.65	1	269.65	271.15	<0.0001
T^2	362.50	1	362.50	364.53	<0.0001
Residual	14.92	15	0.99		
Lack of fit	10.08	10	1.01	1.043	0.51
Pure error	4.83	5	0.97		
Cor total	2421.37	29			
Standard deviation	1.00		R-squared	0.99	
Mean	174.23		Adj R-squared	0.988	
C.V. %	0.57		Preds R-squared	0.973	
Press	65.04		Adeq precision	41.65	

The model F-value of 172.85 implies that the relationship is significant. There is only a 0.01% chance that this large "model F-value" could occur due to noise. Values of "prob>F" less than 0.0500 indicate the relationship terms are significant. In this case, P, B, F, T, PB, PF, PT, BF, BT, FT, P^2, B^2, F^2 and T^2 are significant model terms. Values greater than 0.1000 indicate the relationship terms are not significant. The "lack of fit F-value" of 1.04 implies that the lack of fit is not significant compared to the pure error. There is a 51.40% chance that a large "lack of fit F-value" could occur due to noise. Coefficient of determination "r^2" is used to find how close the predicted and experimental values lie. The value of "r^2" for the above-developed relationship is also presented in Table 5, which indicates high correlation existing between the experimental values and predicted values.

The "Pred. R-squared" of 0.973 is in reasonable agreement with the 'adj R-squared' of 0.988. "Adeq precision" measures the signal to noise ratio. The normal probability plots of the residuals for tensile strength are shown in Fig.4 which reveals the residuals are falling on the straight line, indicating the errors are distributed normally[13]. All the above consideration indicates an excellent adequacy of the developed empirical relationship. Each observed value is compared with the predicted value calculated from the relationship in Fig.5.

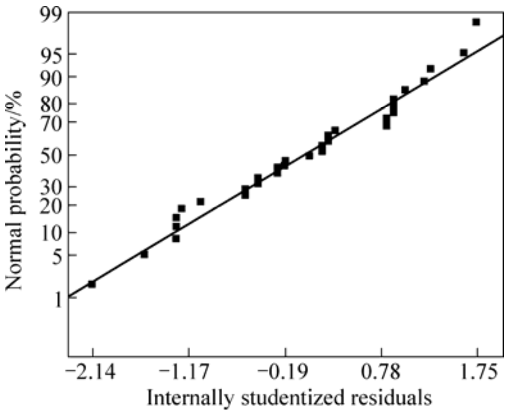

Fig.4 Normal probability plot of residuals

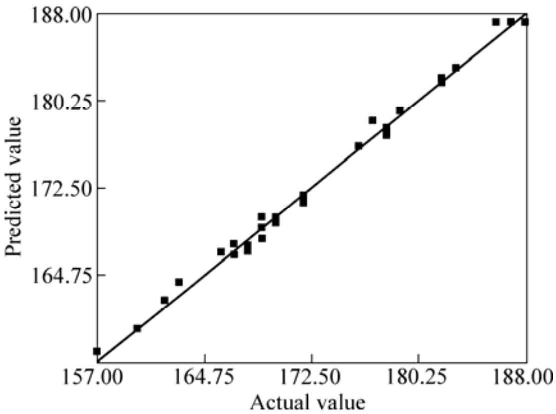

Fig.5 Correlation graph

3 Optimization of PCGTAW parameters

The response surface methodology (RSM) was used as an optimization tool to search the optimum values of the process variables. The empirical relationship developed in the previous section was framed using the coded values. The optimization was done on coded values and then converted to actual values. Design Expert statistical software package was used to optimize the process variables. The optimum values obtained are listed in Table 6. Under the optimum conditions, a maximum tensile strength of 188 MPa was obtained.

Response surfaces were developed for the empirical relationship, taking two parameters in the 'X' and 'Y' axes and response in 'Z' axis. The response surfaces clearly indicate the optimal response point. The optimum tensile strength of PCGTA welded AZ31B magnesium alloy was exhibited by the apex of the response surface, as shown in Fig.6.

Contour plots show distinctive circular mound shape which is indicative of possible independence of factors with response to display the region of optimal factor settings. By generating contour plots using software for response surface analysis, the optimum is located with reasonable accuracy by characterizing the shape of the surface. If a contour patterning of circular shaped contour occurs, it tends to suggest the independence of factor effects while elliptical contours may indicate factor interactions[14]. The optimum response for PCGTA welded AZ31B magnesium alloy is shown in Fig.7.

Table 6 Optimised PCGTAW process parameters

Parameter	Optimized parameter	
	Predicted by RSM	Experimental
Peak current/A	204.8	210
Base current/A	77.9	80
Pulse frequency/Hz	6.5	6
Pulse on time/%	45.7	50

4 Analysis of response graphs and contour plots

By generating response graphs and contour plots using Design Expert software for response surface analysis, it is easy to locate the optimum conditions with reasonable precision.

Fig.6(a) shows the three dimensional response surface plot for the response tensile strength obtained from the regression model, assuming a peak current of 210 A and a base current of 80 A. The optimum tensile strength is exhibited by the apex of the response surface. From the response graph, it is identified that at the peak current of 210 A, the tensile strength of PCGTAW joints is higher. The formation of fine equiaxed grains in fusion zone increases the tensile strength of these joints. When the peak current is increased from 210 A, the tensile strength decreases. This is the result of the increased input heat associated with the use of higher peak current. The formation of coarser grains in the fusion zone is responsible for the lower tensile properties of these joints. This phenomenon can be also explained by the change of cooling rate. It is known that an increase in heat input results in slow cooling rate. Moreover, the slower the cooling rate during solidification, the longer the time

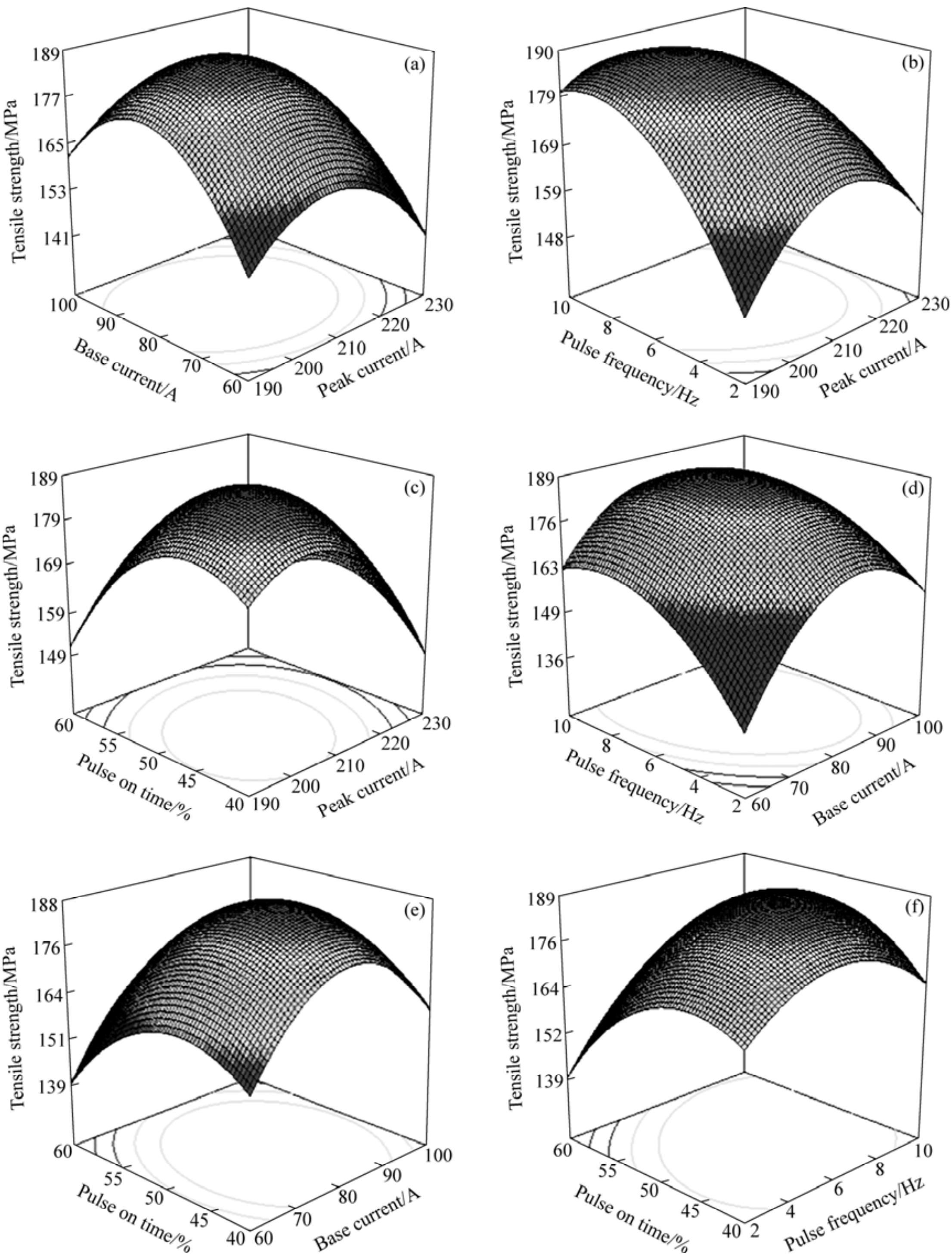

Fig.6 Response graphs for PCGTA welded AZ31B magnesium alloy

available for grain coarsening. In contrast, the decrease in peak current leads to the decrease in heat input, which leads to faster cooling rate and subsequently finer grain size in fusion zone[13].

Fig.6(b) depicts the three dimensional response surface plot for the response tensile strength obtained from the regression model, assuming a pulse frequency of 6 Hz and peak current of 210 A. From the response graph, it is observed that when the pulse frequency is 2 Hz, the tensile strength of PCGTAW joint is lower. When the pulse frequency is increased to 6 Hz, the tensile strength is increased. The finer grain size of fusion zone is responsible for the increase in tensile strength of these joints. At very low frequencies, the effect of pulsing on the weld bead is less obvious compared to that at high frequency pulsing. It is also true that mechanical and thermal disturbances to the weld pool at low frequency of pulsing are expected to be less

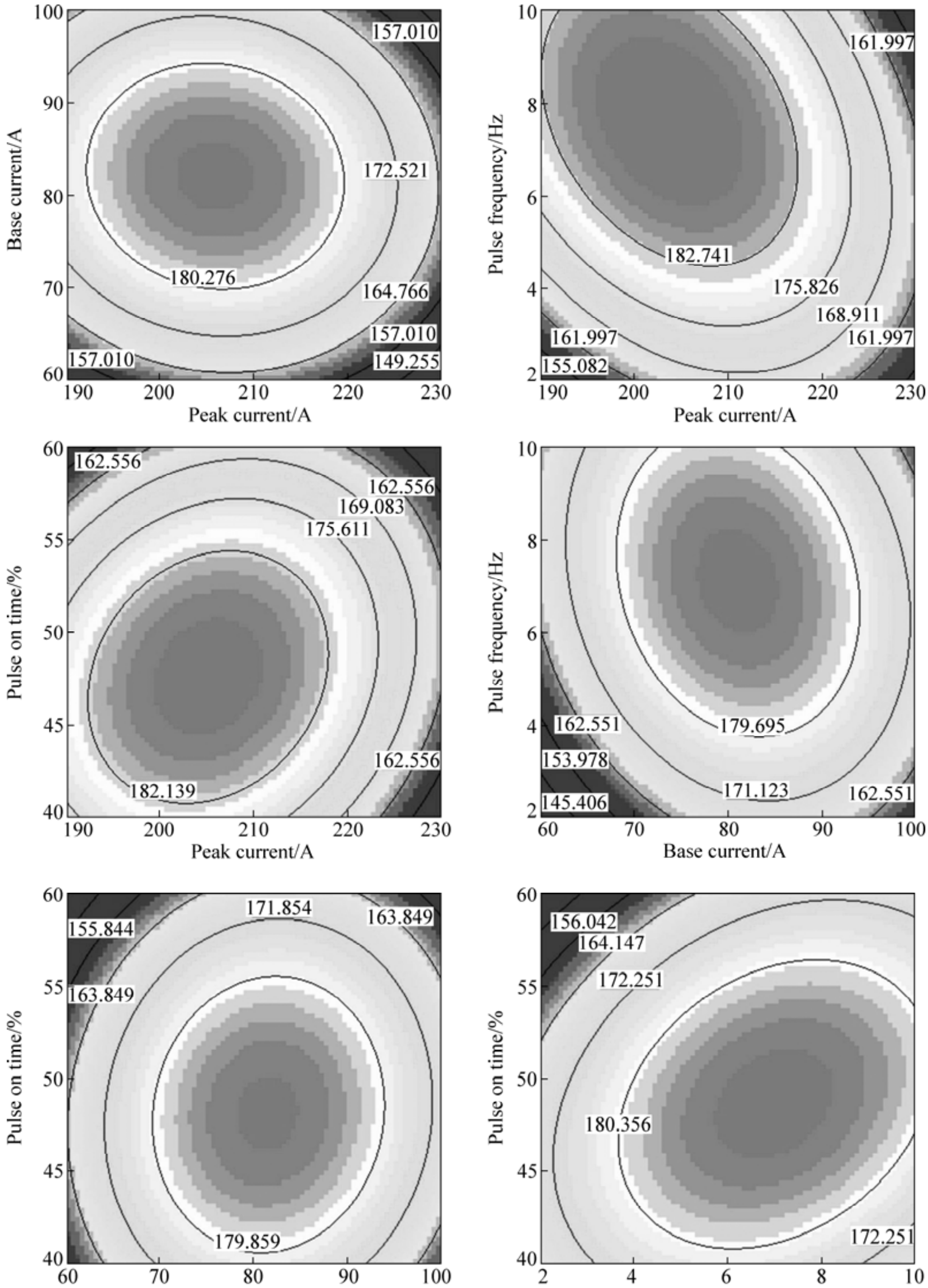

Fig.7 Contour plots for PCGTA welded AZ31B magnesium alloy

intense. At high frequencies, the vibration amplitude and temperature oscillation induced on the weld pool are reduced to a greater extent resulting in reduced effect on the weld pool. Moreover, at high pulse frequency values, the molten pool is agitated violently, resulting in grain refinement in the weld region[15]. Hence, there exists an optimum pulse frequency at which the grain refinement is maximum. In this investigation, the optimum pulse current frequency is found to be 6 Hz.

Fig.6(c) shows the three dimensional response surface plot for the response tensile strength obtained from the regression model, assuming a pulse on time of 50% and peak current of 210 A. From the response graph, it is identified that at the pulse on time of 50%, the tensile strength of PCGTAW joints is higher. The fine grains observed in the fusion zone may be responsible for higher tensile strength of these joints. This is mainly due to the optimum heat input. The pulse on time increases further, which promotes the grain growth on the weld region. This is because as the pulse on time increases, the period from the start of a pulse to the end of the base time also increases. When the pulsing time is increased, the welding heat has more time to conduct into the fusion zone, which promotes grain coarsening[16]. The grains in fusion zone get coarser, with increasing pulse on time, and the tensile strength of these joints decreases.

Fig.6(d) shows the three dimensional response surface plot for the response tensile strength obtained from the regression model, assuming a base current of 80 A and a pulse frequency of 6 Hz. From the response graph, it is observed that when the base current is 80 A, the tensile strength of PCGTAW joint is higher. The fine grains observed in the fusion zone due to optimum heat input may be responsible for the better tensile strength of these joints. When the pulse frequency increases to 100 A, the tensile strength decreases. The grain coarsening deteriorates the tensile properties of these joints.

Fig.6(e) presents the three dimensional response surface plot for the response tensile strength obtained from the regression model, assuming a base current of 80 A and pulse on time of 50 %. From the response graph, it is observed that when the base current is 80 A, the tensile strength of PCGTAW joint is higher.

Fig.6(f) shows the three dimensional response surface plot for the response tensile strength obtained from the regression model, assuming a pulse frequency of 6 Hz and a pulse on time of 50%. From the response graph, it is observed that when the pulse frequency is 6 Hz, the tensile strength of PCGTAW joint is high. The fine grains observed in the fusion zone due to optimum heat input may be responsible for the better tensile

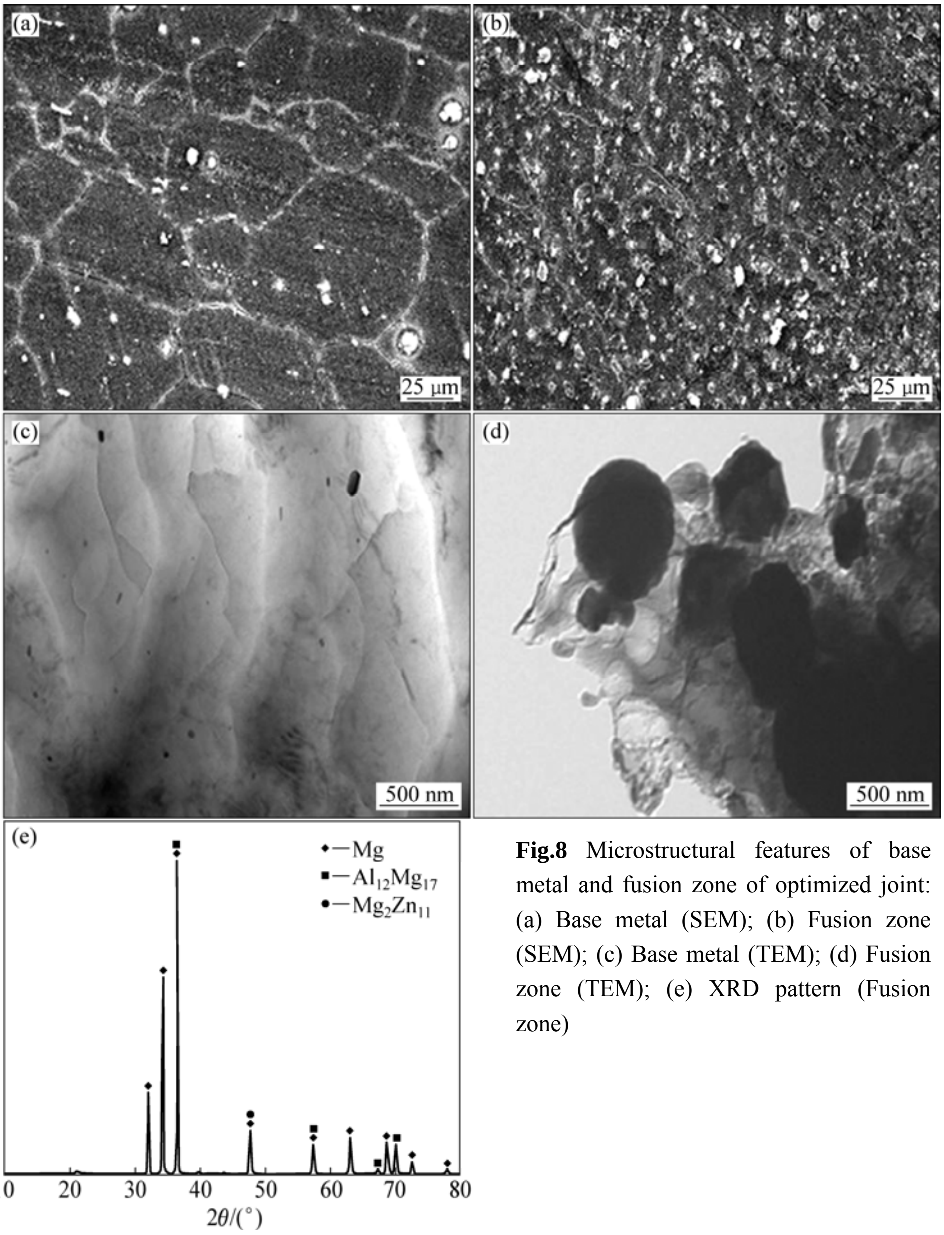

Fig.8 Microstructural features of base metal and fusion zone of optimized joint: (a) Base metal (SEM); (b) Fusion zone (SEM); (c) Base metal (TEM); (d) Fusion zone (TEM); (e) XRD pattern (Fusion zone)

strength of these joints.

The SEM and TEM micrographs of the base metal and fusion zone of the joints made with a peak current of 210 A, base current of 80 A, pulse frequency of 6 Hz and pulse on time of 50 % are shown in Fig.8. The formation of fine grains in weld region is the main reason for higher tensile strength of the above joint. Furthermore, evidence of a large number of precipitated particles is observed in the fusion zone and the concentration of precipitates is moderate, which is also one of the reasons for higher tensile properties of these joints compared to others. The XRD pattern presented in Fig.8(e) confirms the presence of $Al_{12}Mg_{17}$ precipitates in fusion zone along with the traces of Mg_2Zn_{11}.

From the contour plot in Fig.7(a), for optimum tensile strength of PCGTAW AZ31B magnesium alloy, the tensile strength is more sensitive to change in peak current than in the base current. From the contour plot in Fig.7(b), it can be seen that the tensile strength is more sensitive to changes in pulse frequency than in peak current. From Fig.7(c), it can be seen that the tensile strength is more sensitive to the change in peak current than in pulse on time. From Fig.7(d), it can be seen that the tensile strength is more sensitive to change in impulse frequency than in base current. From Fig.7(e), it can be seen that the tensile strength is more sensitive to change in pulse on time than in base current. From Fig.7(f), it can be seen that the tensile strength is more sensitive to change in pulse frequency than in pulse on time.

5 Conclusions

1) An empirical relationship was developed to predict tensile strength of pulsed current gas tungsten arc welded AZ31B magnesium alloy using response surface methodology. The developed relationship can be effectively used to predict the tensile strength of pulsed current gas tungsten arc welded joints at 95% confidence level.

2) A maximum tensile strength of 188 MPa was obtained under the welding condition of peak current of 210 A, base current of 80 A, pulse frequency of 6 Hz and pulse on time of 50%, which is the optimum PCGTA welding condition for AZ31B magnesium alloy and confirmed by RSM.

3) Pulse frequency has the greatest influence on tensile strength, followed by peak current, pulse on time and base current.

References

[1] MUNITZ C, COTLER A, KOHN S G. Mechanical properties and microstructure of gas tungsten arc welded magnesium AZ91D plates [J]. Mater Sci Eng A, 2001, 302: 68−73.

[2] SU S F, HUANG J C, LIN H K, HO N J. Electron-beam welding behavior in Mg-Al-based alloys [J]. Metall Mater Trans A, 2002, 33: 1461−1473.

[3] LEE W B, KIM J W, YEON Y M, JUNG S B. The joint characteristics of friction stir welded AZ91D magnesium alloy [J]. Mater Trans, 2003: 44: 917−923.

[4] ASM International. Welding, brazing and soldering [M]//ASM handbook, vol 6. Ohio: Materials Park, 1993.

[5] LANCASTER J F. Metallurgy of welding [M]. 6th ed. Abington: Cambridge, 1999.

[6] MYERS R H, MONTGOMERY D H. Response surface methodology [M]. USA: John Wiley & Sons, 1995, 705.

[7] LIU Li-ming, DONG Chang-fu. Gas tungsten-arc filler welding of AZ31 magnesium alloy [J]. Mater Lett, 2006, 60: 2194−2197.

[8] BEN-HAMU G, ELIEZER D, CROSS C E, BÖLLINGHAUS T H. The relation between microstructure and corrosion behavior of GTA welded AZ31B magnesium sheet [J]. Mater Sci Eng A, 2007: 452−453: 210−218.

[9] LIU L M, ZHANG Z D, SONG G, WANG L. Mechanism and microstructure of oxide fluxes for gas tungsten arc welding of magnesium alloy [J]. Metall Mater Trans A, 2006, 38: 649−658.

[10] SHEN J, YOU G Q, LONG S Y, PAN F S. Abnormal macropore formation during double-sided gas tungsten arc welding of magnesium AZ91D alloy [J]. Mater Charact, 2008, 59(8): 1059−1065.

[11] BALASUBRAMANIAN M, JAYABALAN V, BALASUBRAMANIAN V. Developing mathematical models to predict grain size and hardness of argon tungsten pulse current arc welded titanium alloy [J]. Journal of Materials Processing Technology, 2008, 196(1−3): 222−229.

[12] BOX G E P, HUNTER W H, HUNTER J S. Statistics for experiments [M]. New York: John Wiley Publications, 1978.

[13] KUMAR S, KUMAR P, SHAN H S. Effect of evaporative casting process parameters on the surface roughness of Al-7%Si alloy castings [J]. J Mater Proc Techno, 2007, 182: 615−623.

[14] MONTGOMERY D C. Design and analysis of experiments [M]. New York: John Wiley & Sons, 2001.

[15] KOU S, LE Y. Nucleation mechanism and grain refining of weld metal [J]. Weld J, 1986: 65−70.

[16] SENTHIL T, KUMAR T, BALASUBRAMANIAN V, SANAVULLAH M Y. Influences of pulsed current tungsten inert gas welding parameters on the tensile properties of AA 6061 aluminium alloy [J]. Materials and Design, 2007, 28: 2080−2092.

[17] BALASUBRAMANIAN V, JAYABALAN V, BALASUBRAMANIAN M. Effect of current pulsing on tensile properties of titanium alloy [J]. Materials and Design, 2008, 29: 1459−1466.

AZ31B 镁合金的脉冲电流气体保护钨极焊过程参数优化

G. PADMANABAN, V. BALASUBRAMANIAN

Center for Materials Joining and Research (CEMAJOR), Department of Manufacturing Engineering,
Annamalai University, Annamalainagar−608 002. Tamil Nadu, India

摘　要：建立预测脉冲电流气体保护钨极焊 AZ31B 镁合金接头的拉伸强度经验方程。研究焊接过程参数如峰值电流、基础电流、脉冲频率和脉冲时间对焊接接头的影响。试验设计了一个四因素五水平的正交实验。建立的经验方程能够有效地预测脉冲电流钨电极惰性气体保护焊 AZ31B 镁合金的焊缝拉伸强度，可信度为 95%。结果表明，脉冲频率对拉伸强度的影响最大，其次是峰值电流、脉冲时间和基电流。

关键词：AZ31B 镁合金；脉冲电流气体保护钨极焊；响应面方法；优化；拉伸强度

(Edited by FANG Jing-hua)